SOFIA, 2013 VOLUME 7 ISSN 1314-0078

ANNUAL JOURNAL OF ELECTRONICS

Technical University of Sofia

Faculty of Electronic
Engineering and Technologies

ANNUAL JOURNAL OF ELECTRONICS

The Journal is issued by the FACULTY OF ELECTRONIC ENGINEERING AND TECHNOLOGIES, TECHNICAL UNIVERSITY of SOFIA, BULGARIA.

The Journal includes the selected papers from the International Scientific Conference Electronics'13, held on 18-20 September 2013 in Sozopol, Science Days of Technical University of Sofia, Bulgaria.

Sponsored by:
TU – SOFIA, project 131ДН0014-03
Faculty of Electronic Engineering and Technologies, TU – Sofia
IEEE Bulgaria Section
IEEE ED/CPMT/MTT/AP Chapter Sofia
IEEE CAS/SSCS Chapter Sofia

CONTENTS

Pandiev I., Analysis and Design of VFOA-Based Small-Signal Amplifier Circuits	1
Djamiykov T. and K. Asparuhova, Random Signals Generation for Computer Analysis of Optoelectronic Circuits	5
Todorov T., Simulink Modelling and Design of FPAA Prototype for Studying of Modified Van der Pol Equation Using Melnikov Theory	9
Petrov B., Application of CPLD for Digital Control of Power Converters	13
Kovacheva M., El. Stoimenov and P. Yakimov, FPGA-based Model of Incremental Rotary Encoder	17
Vandenbussche J.-J., P. Lee and J. Peuteman, Design of an FPGA Based TV-tuner Test Bench Using MFIR Structures	21
Nenkov J. and L. Jordanova, P2P Video-on-Demand Services through Cable Television Networks	26
Yordanov R. and I. Ucherdzhiev, Education in Electronics Using Students as Mediators	30
Goranova M., G. Georgiev, T. Vasileva and L. Stoyanova, SOA-based Scientific Data Management and Visualization System	34
Stoyanova L. and M. Goranova, The Assessment Methods in the Web Services Based Test System	38
Shoshkov Ts. and G. Mihov, Simulink Implementation of the Subtraction Procedure for Interferences Removal from ECG	42
Kostadinov A., Field-Programmable-Logic Device Education	46
Catteeuw W., H. Hallez and J. Boydens, Reliability Study of the Hitachi H34C Accelerometer in Wireless Body Area Networks for Fall Detection	50
Dotsinsky I., T. Stoyanov and Ts. Mudrov, Power-line Frequency Monitoring Using Component of the Subtraction Procedure for ECG Processing	54
Iliev I. and S. Tabakov, High-risk Patients Telemetry by ECG Sonification	57
Jekova I., V. Krasteva, G. Georgiev, L. Todorova, P. Vassilev and M. Matveev, Decision Support System for Prediction of the Weaning Outcome from Mechanical Ventilation	60
Dobrev D. and T. Neycheva, Digital Lock-in Technique for Input Impedance Balance in Two-electrode Biosignal Amplifiers	64
Dobrev D. and T. Neycheva, Analog Approach for Common Mode Impedance Balance in Two-electrode Biosignal Amplifiers	68
Witte N., R. Vincke, S. Landschoot, E. Steegmans and J. Boydens, Comparing Dual-Core SMP/AMP Performance on a Telecom Architecture	72
Cordemans P., J. Boydens and E. Steegmans, Task Parallel Paradigms: a Comparative Case Study	76
Vincke R., N. Witte, S. Landschoot, E. Steegmans and J. Boydens, Algorithm	80

Parallelization using Software Design Patterns
Vincke R., A. Messiaen and J. Boydens, Hybrid FPGA/Multi-core CPUs for Industrial Applications 84
Cholakov A., Y. Slavov and P. Manoilov, Design and Implementation of a Pipelined Image Processing FPGA Architecture 87
Karakehayov Z., Out of Order Execution for Dynamic Power Management 91
Ivanov R. and L. Bogdanov, Dynamic Frequency Scaling in Embedded Systems 95
Neshev I., Extensible Serial Protocol Specification 99
Stoimenov E., RF Transceiver with Reduced Size and Weight Used in Wild Tracking System 101
Bliznakovski Vl., Z. Kokolanski and Cv. Gavrovski, Improvement of Measuring System for Monitoring of Moving Steel Rope Conditions 105
Hensel St., T. Strauß and M. Marinov, Non-contact and Slipless Velocity Estimation for Rail Vehicles with Eddy Current Sensors 109
Lazarov Ts. and T. Djamiykov, Utilizing CMOS Image Sensor Embedded Functions to Reduce Number of Pixels in a Frame 113
Lyubomirov Sl., St. Ovcharov and St. Vichev, Microprocessor Module to a Protection Relay for Determining the Distance to the Short Circuit 116
Iovev A., P. Yakimov and N. Tuliev, Investigation and Development of Differential Temperature Controller for Drain Back Solar Systems 120
Trifonova T., V. Markova and V. Draganov, Development of Smart Sensor for Monitoring Relative Air Humidity in the Workplace 124
Ivanov S. and G. Nikolov, Intelligent System for Capacitance Measurements 128
Marinov M., G. Nikolov, T. Djamiykov and St. Hensel, Accuracy Improvement of CO2 Concentration Measurement 132
Djermanova N., Zh. Kiss'ovski, D. Mitev, V. Vachkov and P. Georgiev, Measuring and Controlling of Carbon Nanostructures Deposition Temperature in Miniature Microwave Surface Wave Discharge 136
Andonova A. and D. Todorov, Thermographic NDT System 139
Popov E., Three-Dimensional Characteristics of a Current Fed Inverter with Complex Type of Load Supplied by a Constant Input Current Source 144
Mareva D., D. Yudov and E. Marev, Simulation Research of Resonant Inverters for Induction Heating of Fluids 148
Bankov N., Al. Vuchev and Y. Madankov, Design Methodology for High Voltage Resonant DC/DC Converter for CO2 Laser Power Supply 152
Vuchev Al., N. Bankov and Y. Madankov, Load Characteristics of High Voltage Resonant DC/DC Converter 156
Spirov D. and N. Komitov, Investigations of Induction Motor Drive System with Input Power Factor Correction Circuit 160
Mihov V. and E. Dinkov, Battery Management System for Multi CellApplications, Using Common HF-L Link 164
Mashkov P., B. Gyoch, H. Beloev and St. Penchev, LEDs' Thermal Loading Investigations in a High Luminous Flux Lamp 168
Vainshtein S., G. Duan and J. Kostamovaara, How High-speed Transient in a Si Avalanche Transistor Can be Improved by Smart Chip Design 172

Gieva El., R. Rusev, P. Goranov, G. Angelov, R. Radonov and M. Hristov, Microelectronic Circuit with Operational Amplifiers Imitating Hydrogen Bonding Network Behaviour 176
Brusev T., Buck Converter Modeling with MATLAB Simulink 180
Brusev T. and B. Nikolova, Control System Modeling for DC-DC Converter 184
Yordanov R., Choosing HIC and MCM Optimal Technological Solution Related to Education in Microelectronics 188
Yordanov R., G. Dimitrov and I. Yordanova, Creating and Usage of 3D Models for the Purpose of Education in Microelectronics 192
Spasov G., Correcting in Auger Electron Spectroscopy 196
Spasov G., Comparing Quantitative Auger Analysis 200
Tzaneva B., Electrochemical and Electroless Deposition of Metal in Anodic Aluminium Oxide Nanoporous Template 204
Delibozov N., R. Radonov and M. Hristov, Design Kit Creation for a Novel MEMS Technology 207
Denishev K., Considerations, Technological Design and Results from the Work on "Air-Bridges" Preparation for Microwave and MEMS Applications 211
Denishev K., Investigation and Design of Angular Motion Magnetic MEMS Actuator 215
Andreev Sv., Method for Metallization of Solder Resist on a PCB Substrate 219
Shindov P., St. Zahariev, T. Anastasova, V. Serbezov and M. Zaharieva, Deposition of CdSSe Layers by Three-Electrode Sputtering 223
Gyoch B., P. Mashkov and St. Penchev, Properties' Worsening Analysis of Multilayer Antireflection Coatings for the Visible Spectral Region 227
Aleksandrova M., Electrical Characterization of Flexible Organic Electroluminescent Devices by Impedance Measurement 231

Control System Modeling for DC-DC Converter

Tihomir Sashev Brusev and Boyanka Marinova Nikolova

Abstract - **DC-DC converters are part of many electronic equipment because energy consumption and power management became important part of whole system design. They are used in battery powered sensor's applications in industrial, automotive, measurement, medical applications etc. Design of voltage regulators could be faster if they are investigated on the high level as a block circuit. This paper presents modeling of control system of buck converter using MATLAB Simulink. The received simulation results can be used as a base for integrated circuits (IC) dc-dc converter design at low transistor's level.**

Keywords – **Battery Powered Sensors, Energy Optimization, Modeling, MATLAB Simulink, Cadence**

I. INTRODUCTION

DC-DC converters improve efficient use of energy of the electronic devices. Therefore they became important part of many types of equipment, such like battery powered sensor's systems, handheld devices, mobile phones etc. Their big advantage compare to linear regulator is that they can ensure higher efficiency η when difference between input and output voltage is high.

In the modern electronic systems the implementation of different type of sensors, such like temperature, humidity and pressure sensors, is dramatically increased. They are widely used everywhere in the measurement, automotive, industrial, medical, air conditioning systems etc. Based on the new MEMS technologies they have unique features, small sizes, low power consumptions, small volumes and not on the last place they are low cost devices.

The usage of those kinds of integrated circuits (IC) improves the whole system's properties and abilities. For example in the air conditioning system they can ensure high efficiency work and detecting problems in the mechanical parts. Those devices could inform driver for pressure in the car's tires – tire pressure monitoring system (TPMS) sensors. Another field of applications is altitude sensors in the aircrafts, blood pressure in medicine, petroleum industry and so on. One application of temperature and humidity sensors for example is in the home weather stations.

Efficient work of those devices is connected with energy optimization and proper power supply consumption. Most of them are battery powered sensors. In those cases we need high efficient dc-dc converter in order to save battery life and the system run time. In some of the applications energy independent measurement equipment are needed. For example this could be temperature and humidity sensors used in medical environments.

Control system of dc-dc converters is important part of whole regulator. Proper design could help to be minimized losses and to be improved overall efficiency η. Using block diagram simulations software behavior of the separate circuits could be predicted.

This paper presents modeling of control system of buck dc-dc converter used in the battery powered sensor nodes. The basic principles of operation of pressure, temperature and humidity sensors are given in Section II. This section includes also short explanation about low power dc-dc converter system designed on CMOS process. The control system of buck converter is modeled and analyzed with MATLAB Simulink. The received results are presented in Section III. They can be used for dc-dc regulator system design at low transistor's level.

II. PRESSURE, TEMPERATURE, HUMIDITY SENSORS AND BUCK DC-DC CONVERTER

One of most popular applications of pressure sensors nowadays is in the automotive industry as a tire pressure monitoring systems (TPMS). The block diagram shown in Figure 1 presented part of used modules which are pressure sensor, temperature sensor, radio frequency (RF) transmitter, microcontroller (MCU), and analog to digital converter (ADC).

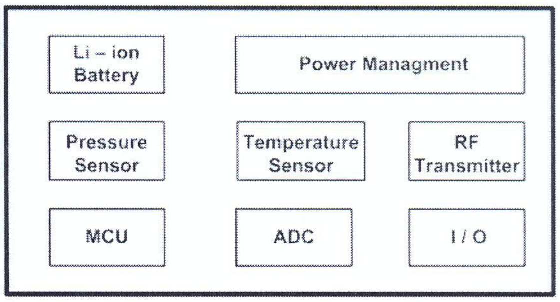

FIGURE 1. TPMS BLOCK DIAGRAM.

The pressure sensors are mounted directly on the tires of the cars. The information is transmitted to the vehicle using radio-frequency technology [2]. The electronic modules inside the tires are powered from Lithium-Ion battery. Typical voltage of such cells is 3.6 V.

Some of the modules used in TPMS operate at lower than the battery voltage. For efficient use of energy from the battery proper power management is needed. This function can be performed by switching-mode dc-dc converter [3].

T. Brusev is with the Department of Technology and Management of Communication Systems", Faculty of Telecommunications, Technical University of Sofia, Kl. Ohridski 8, 1797 Sofia, Bulgaria, E-mail: brusev@ecad.tu-sofia.bg.

B. Nikolova is with the Department of Technology and Management of Communication Systems, Faculty of Telecommunications, Technical University of Sofia, Kl. Ohridski 8, 1797 Sofia, Bulgaria, E-mail: bnikol@tu-sofia.bg

A. Main Characteristics of Integrated Sensors

The main building blocks of intergraded sensor are shown on the Figure 2. The sensor element can be realized by MEMS technology (piesoresistive pressure sensor) or can be thin film capacitor or resistor (for humidity or temperature measurement). Usually the block that converts physical phenomena into voltage consists of current source, voltage divider and differential amplifier [1, 4, 5].

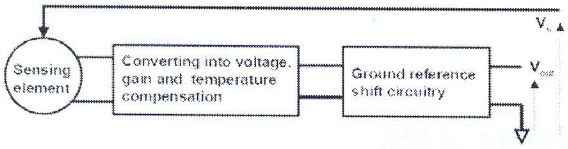

FIGURE 2. THE BUILDING BLOCKS OF INTEGRATED SENSOR.

The transfer function establishes dependence between the electrical signal *V* produced by the sensor and the stimulus (physical phenomena) *P*. That function may be a simple linear relationship or a nonlinear dependence, (e.g., logarithmic, exponential, or power function). Most sensors are inherently analogue and must have their signals digitized by an ADC before they can be used in integrated electronic systems. One of the important advantages of integrated sensor is the capability of ratiometric connection with ADC. A connection is ratiometric if the sensor's output voltage V_{OUT} is directly proportional to its supply voltage V_S. The ratiometric characteristics of this sensors and ADCs can be used to improve accuracy while simultaneously reducing overall component count, lowering cost, and reducing board space.

A dynamic range of stimuli, which may be converted by a sensor, is called a span or an input full scale. It represents the highest possible input value that can be applied to the sensor without causing an unacceptably large inaccuracy. Full-scale output is the algebraic difference between the electrical output signals measured with maximum input stimulus and the lowest input stimulus applied. This must include all deviations from the ideal transfer function.

Under static conditions, a sensor is fully described by its transfer function, span and calibration. However, when an input stimulus varies, a sensor response generally does not follow with perfect fidelity. Then, the sensor's time-dependent characteristics can be studied by evaluating the differential equation.

The calibration error is inaccuracy permitted by a manufacturer when a sensor is calibrated in the factory. This error is of a systematic nature, meaning that it is added to all possible real transfer functions. It shifts the accuracy of transduction for each stimulus point by a constant. This error is not necessarily uniform over the range and may change depending on the type of error in the calibration [1, 4, 6].

B. Pressure, Temperature and Humidity Sensors

A pressure sensor operating principle is based on the conversion of a result of the pressure exertion on a sensitive element into an electrical signal. The pressure results in the displacement or deformation of an element have a defined surface area. Thus, a pressure measurement may be reduced to a measurement of a displacement or force, which results from a displacement [1, 6].

Most used pressure sensor types are piezoresistive, capacitive, piezoelectric. Piezoresistive types of sensors use the piezoresistive effect of bonded or formed strain gauges to detect strain due to applied pressure. This is the most commonly employed sensing technology for general purpose pressure measurement. Generally, these technologies are suited to measure absolute, gauge and differential pressures.

Capacitive types of sensors use a diaphragm and pressure cavity to create changes in capacitance to detect strain due to applied pressure. Common technologies use metal, ceramic, and silicon diaphragms. Generally, these technologies are most applied to low pressures.

Piezoelectric types of sensors use the piezoelectric effect in certain materials such as quartz to measure the strain upon the sensing mechanism due to pressure. This technology is commonly employed for the measurement of high dynamic pressures.

Modern pressure sensors manufactured using innovative MEMS technology to provide power supply voltage from 1.71 V to 3.6 V and supply current of about 30 μA, therefore they are suited for battery operated systems [7].

The most common temperature sensors that are used to perform this task are: thermocouples, resistive temperature detectors (RTDs), thermistors and silicon temperature sensors, which are primarily classified according to their output-signaling method. Those technologies are used for specific temperature ranges and environmental conditions.

Local temperature sensors provide their die temperature in either analog or digital format. Outputs of analog temperature sensors are voltage or current, which change depending on the die temperature. Usually, the output of the analog sensor is connected to an analog-to-digital converter (ADC) to provide the temperature information in the digital domain. This ADC can be discrete or integrated in the microcontroller or other devices.

The output voltage of an analog temperature sensor cannot exceed the input supply voltage. Therefore, to use an analog temperature sensor from –50 °C to +150 °C with a supply voltage of 1.8V nominal, the maximum gain that analog sensor can have is 6 mV/°C. To handle this gain and monitor the temperature accurately, a high-resolution ADC needs to be used [1, 8].

There are analog temperature sensors [8] which guaranteed to operate from a 1.8V supply voltage and 9 μA supply current. That makes them ideal for portable two-cell, battery-powered systems and single-cell, Li-Ion systems.

Humidity sensors can be capacitive, resistive and thermal conductive. In capacitive humidity sensors, the effect of humidity on the change in dielectric constant of a polymer or metal oxide material is measured. With calibration, these sensors can have an accuracy of ±3% RH in the range 5–95% RH. Without calibration the accuracy of these sensors, can decrease to ±20% [1, 5].

In resistive humidity sensors, the change in electrical resistance of a material due to humidity is measured. Resistive sensors are less sensitive than capacitive sensors -

the change in material resistance is less, so they require more complex circuitry. The robustness and accuracy against condensation highly depend on the chosen resistive material. Robust, condensation-resistant sensors exist with an accuracy of up to ±3-4% RH.

Some types of relative humidity sensor are laser trimmed, thermoset polymer capacitive sensing element with on-chip integrated signal conditioning. It has a typical current draw of only 200 μA, whereby it is ideally suited for low drain, battery operated systems.

Often the consumption of combination of these three types of sensors, and microcontroller is about 10÷12 mA. In case of battery powered device, one of the most important things to increase battery live is optimization of power supply unit.

C. Buck DC-DC Converter

The block diagram of the switching-mode dc-dc buck converter system using standard pulse width modulation (PWM) control method is shown in Figure 3. The NMOS and PMOS transistors, which are forming the power stage, are synchronously controlled in a way that when one of the transistors is switched-on the other is switched-off. Using high switching frequency f_s is the key to possible integration of filter components, respectively inductor L and capacitor C. In such way the sizes, volume and price of whole dc-dc converter could be minimized.

The block circuit shown in Figure 3 is designed on CMOS technology using Cadence. The nominal supply voltage of the converter is 3.6 V and steps-down to 1.2 V. The input voltage is the same like battery voltage of tire pressure monitoring systems TPMS block diagram illustrated in Figure 1. Some of the presented modules work at these voltage levels.

The system consists of bandgap reference, error amplifier, ramp generator, comparator, buffer and power buck stage. The power losses in the controlling stages are minimized in order to improve the overall converter efficiency η, which is one the most important parameters of the voltage regulators.

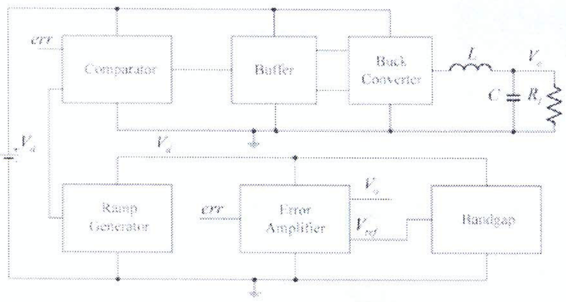

FIGURE 3. PULSE WIDTH MODULATION (PWM) CONTROL SYSTEM OF BUCK CONVERTER.

DC-DC buck converter is designed to operate at switching frequency f_s equal 150 MHz. The reason for using high f_s is an opportunity for integration of the filter. In Figure 4 is illustrated output voltage V_o of the whole regulator including control system as function of the load current I_{Load}.

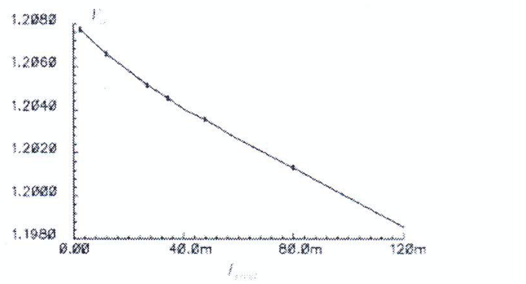

FIGURE 4. OUTPUT VOLTAGE V_O AS A FUNCTION OF LOAD CURRENT I_{LOAD} OF THE BUCK CONVERTRE DESIGNED ON CMOS TECHNOLOGY.

The investigations and analysis of the whole system which have to be made at low transistor's level take long time. For example, one simulation at that high switching frequency could take one day.

III. CONTROL SYSTEM OF BUCK CONVERTER MODELING USING MATLAB SIMULINK

DC-DC converter system can be designed as block circuit on the top behavioral level using. Top-down method is effective way to save time during the whole circuit's design. The modeling of control system of dc-dc converter, shown in Figure 3, would accelerate the design of the converter.

The block circuit of the designed buck dc-dc converter is investigated and analyzed using MATLAB Simulink.

The ramp generator is a part of the regulation system, which performs the pulse-width modulation (PWM) control. This stage determines the switching frequency f_s of the buck converter. The whole system behavior is simulated and investigated on the top level with MATLAB Simulink. The pulse-width modulation (PWM) control circuit modeled with MATLAB Simulink is shown in Figure 5 [9].

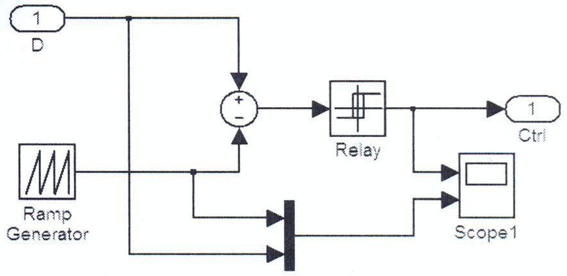

FIGURE 5. EQUIVALENT MODEL OF PWM CONTROL CIRCUIT.

The received results for pulse-width modulation PWM control pulses, which regulate transistors in the power stage of the dc-dc regulator, when the system is in regulation, are shown in Figure 6. In same picture are presented output voltages of ramp generate and the constant dc level of error amplifier.

The switching frequency of the modeled control system of buck converter is f_s=150 MHz, while input and output voltages are respectively V_d=3.6 V and V_o=1.2 V. The output voltage of buck converter system modeled with MATLAB Simulink is shown in Figure 7.

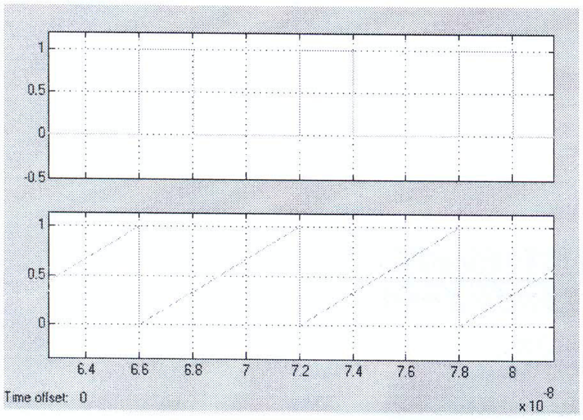

FIGURE 6. CONTROL PULSES OF BUCK CONVERTER AND OUTPUT VOLTAGE OF RAMP GENERATOR MODELED WITH MATLAB SIMULINK.

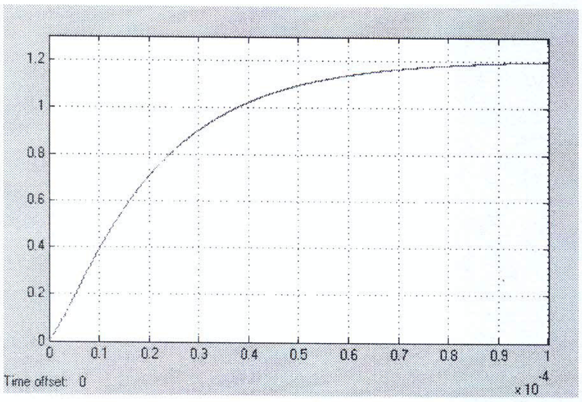

FIGURE 7. OUTPUT VOLTAGE V_O OF THE BUCK DC-DC CONVERTER SYSTEM SIMULATED WITH MATLAB SIMULINK.

The received results from investigation of the control system of buck converter with MATLAB Simulink, could be used as a base for further investigation at the low transistor's level. That topology of buck dc-dc converter has been designed for IC application using CMOS technologies.

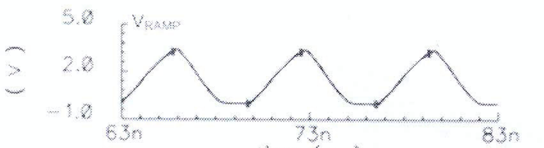

FIGURE 8. OUTPUT VOLTAGE OF RAMP GENERATOR V_{RAMP} OF BUCK CONVERTER SYSTEM DESIGNED WITH CADENCE.

In Figure 8 is illustrated output voltage of ramp generator of buck converter system designed with Cadence presented in Figure 3. The results show that waveform of sawtooth signal is not the same like this from Figure 6. The reason is that when block diagram simulation software is used some of the parasitic components of the real transistors, resistors and capacitors are difficult to be predicted. But behavior of the whole system can be predicted with good approximation. On the other hand simulations of the equivalent model, is much faster compared to the transistor's level analysis and investigations of the block circuits.

IV. CONCLUSION

In this paper is presented modeling of control system buck dc-dc converter which perform pulse-width modulation (PWM), using MATLAB Simulink. The investigations are oriented to battery powered sensor nodes. The basic principles of operations of pressure, temperature, humidity sensors and buck dc-dc converter are given. Energy optimization could increase the system run time. The received simulation results, which could be the base for further design at low transistor' level, are given.

ACKNOWLEDGEMENT

The research described in this paper was carried out within the framework of UNIK Project DUNK – 01/03 – 12.2009.

REFERENCES

[1] Wilson J. S. , *Sensor Technology Handbook*, Elsevier Inc., ISBN: 0-7506-7729-5, 2005.

[2] Liu Y., H. Binghua, S. Jianchun, Y. Yuan, *Design and Implementation of TPMS Based on Wireless Sensor Network*, IEEE Intelligent System Design and Engineering Application (ISDEA), 13 – 14 Oct. 2010 International Conference, pp. 518-523.

[3] A. J. Stratakos, S. R. Sanders, and R. W. Broderson, *A low-voltage CMOS dc–dc converter for a portable battery-operated system*, Power Electronics Specialists Conf., vol. 1, June 1994, pp. 619–626

[4] Nikolova, B., G. Nikolov, M. Hristov. *Analogue Behavioural Modelling of Integrated Sensors*. The 2006 International Conference on Computer Engineering & Systems (ICCES'06), ISBN 1-4244-0271-9, pp. 107-112, Cairo, Egipt, November 5-7, 2006.

[5] St. Beeby, G. Ensell, M. Kraft, N. White, *MEMS mechanical sensors*, Artech House Inc., ISBN 1-58053-536-4, 2004.

[6] J. Fraden, *Handbook of modern sensors: physics, designs, and applications*, Springer-Verlag New York, Inc., 3rd ed., ISBN 0-387-00750-4, 2004.

[7] STMicroelectronics, *LPS331AP MEMS pressure sensor: 260-1260 mbar absolute digital output barometer*, Datasheet, March 2012.

[8] Texas Instruments, *LM94021,LM94022Temperature sensor solutions for low-voltage systems*, Datasheet, 2012.

[9] http://ecee.colorado.edu